

available at [www.sciencedirect.com](http://www.sciencedirect.com)journal homepage: [www.elsevier.com/locate/biochempharm](http://www.elsevier.com/locate/biochempharm)

# Glyoxal markedly compromises hepatocyte resistance to hydrogen peroxide

Nandita Shangari<sup>a</sup>, Tom S. Chan<sup>b</sup>, Marija Popovic<sup>a</sup>, Peter J. O'Brien<sup>a,\*</sup>

<sup>a</sup> Department of Pharmaceutical Sciences, University of Toronto, 19 Russell St, Toronto, Ont., Canada M5S 2S2

<sup>b</sup> Centre de Recherche, CHUM, Hôpital Saint-Luc, 264 Boul. René Lévesque Est, Montréal, Que., Canada H2X 1P1

## ARTICLE INFO

### Article history:

Received 15 January 2006

Accepted 21 February 2006

### Keywords:

$\alpha$ -Oxoaldehydes

Glyoxal

Oxidative stress

Cytotoxicity

Carbonylation

Reactive oxygen species

Hydrogen peroxide

### Abbreviations:

AGEs, advanced glycation

end-products

DCFH-DA, 2',7'-dichlorofluorescein diacetate

DNFB, 2',4'-dinitrofluorobenzene

DNPH, dinitrophenylhydrazine

G6PDH, glucose-6-phosphate dehydrogenase

H<sub>2</sub>O<sub>2</sub>, hydrogen peroxide

ICDH, isocitrate dehydrogenase

ROS, reactive oxygen species

## ABSTRACT

Glyoxal is an interesting endogenous  $\alpha$ -oxoaldehyde as it originates from pathways that have been linked to various pathologies, including lipid peroxidation, DNA oxidation and glucose autooxidation. In our previous study we showed that the LD<sub>50</sub> of glyoxal towards isolated rat hepatocytes was 5 mM. However, 10  $\mu$ M glyoxal was sufficient to overcome hepatocyte resistance to H<sub>2</sub>O<sub>2</sub>-mediated cytotoxicity. Hepatocyte GSH oxidation, NADPH oxidation, reactive oxygen species formation, DNA oxidation, protein carbonylation and loss of mitochondrial potential were also markedly increased before cytotoxicity ensued. Cytotoxicity was prevented by glyoxal traps, the ferric chelator, desferoxamine, and antioxidants such as quercetin and propyl gallate.

These results suggest there is a powerful relationship between H<sub>2</sub>O<sub>2</sub>-induced oxidative stress and glyoxal which involves an inhibition of the NADPH supply by glyoxal resulting in cytotoxicity caused by H<sub>2</sub>O<sub>2</sub>-induced mitochondrial oxidative stress.

© 2006 Elsevier Inc. All rights reserved.

\* Corresponding author. University of Toronto, Department of Pharmaceutical Sciences, 19 Russell St., Rm 522, Toronto, Ont., Canada M5S 2S2. Tel.: +1 416 978 2716; fax: +1 416 978 8511.

E-mail address: [peter.obrien@utoronto.ca](mailto:peter.obrien@utoronto.ca) (P.J. O'Brien).

0006-2952/\$ – see front matter © 2006 Elsevier Inc. All rights reserved.

doi:10.1016/j.bcp.2006.02.016

## 1. Introduction

Glyoxal and methylglyoxal (MG) toxic effects may contribute to cardiovascular disease, cataractogenesis, muscular disease, complications associated with diabetes mellitus, Alzheimer's and Parkinson's diseases [1–4].

Glyoxal is a reactive  $\alpha$ -oxoaldehyde that originates endogenously from glucose and ascorbate autooxidation, DNA oxidation and lipid peroxidation [3–5]. Furthermore, glyoxal and MG, constitute a significant portion of air-borne carbonyl compounds originating from automotive exhausts [1]. Additionally, cooking food at high temperatures also results in the formation of glyoxals [6]. MG and glyoxal (i.e. glyoxals) are bifunctional alkylating agents that react non-enzymatically with free amino and thiol groups of biomolecules, resulting in the formation of advanced glycation end-products (AGEs) [4]. Glycosylamine protein crosslinks are formed with lysine, while imidazolone derivatives are formed with arginine residues [7,8]. Glyoxals can also react with amino groups of DNA/RNA and lipids [9].

MG and glyoxal can be detoxified endogenously primarily by the glyoxalase system, which converts glyoxal to glycolate and MG to D-lactate in the presence of glutathione (GSH) [10]. Another minor detoxification pathway for glyoxal is catalyzed by reductases such as aldehyde reductase (ALR1), aldose reductase (ALR2) and carbonyl reductase (ALR3). All these enzymes have a broad substrate specificity, are located in the cytosol, and require NADPH or NADH as co-factors [11].

Under conditions of oxidative stress, GSH levels are decreased which impairs glyoxals detoxification [4]. Glyoxals probably through the process of protein glycation residues have been reported to inactivate critical cellular enzymes like  $\alpha$ -ketoglutarate dehydrogenase, thioredoxin reductase, GSH reductase, GSH peroxidase, superoxide dismutase and NADPH supplying dehydrogenases [6]. Therefore, there is an overlapping requirement for reducing equivalents for both antioxidant defense and glyoxal detoxification.

In the present study, we found that low concentrations of glyoxal (10  $\mu$ M) markedly increased  $H_2O_2$ -induced rat hepatocyte GSH oxidation and cytotoxicity. Furthermore, there was also increased reactive oxygen species (ROS) formation, DNA oxidation, protein carbonylation and decreased mitochondrial membrane potential and cellular NADPH levels.

## 2. Materials and methods

Glyoxal (40%, w/v), 2',4'-dinitrofluorobenzene (DNFB), glucose, glucose oxidase, 2',7'-dichlorofluorescein diacetate (DCFDA),  $H_2O_2$  (30%, w/v), dinitrophenylhydrazine (DNPH), 1',2'-diaminobenzene, rhodamine 123, NADPH and trichloroacetic acid (TCA) were purchased from Sigma Chemical Co. (St. Louis, MO).

### 2.1. Animal treatment and hepatocyte preparation

Male Sprague–Dawley rats weighing 275–300 g (Charles River Laboratories) were housed in ventilated plastic cages over PWI 8-16 hardwood bedding. There were 12 air changes per hour, 12-h light photoperiod (lights on at 0800 h) and an environmental temperature of 21–23 °C with a 50–60% relative humidity. The

animals were fed with a normal standard chow diet and water ad libitum. Hepatocytes were isolated from rats by collagenase perfusion of the liver as described by Moldeus et al. [12].

Isolated hepatocytes (10 mL,  $10^6$  cells/mL) were suspended in Krebs–Henseleit buffer (pH 7.4) containing 12.5 mM HEPES in continually rotating 50 mL round bottom flasks, under an atmosphere of 95%  $O_2$  and 5%  $CO_2$  in a 37 °C water bath for 30 min. Glucose (10 mM)/glucose oxidase (1 U/mL;  $H_2O_2$  generating system) was used to generate  $H_2O_2$ . Stock solutions of chemicals were made in  $H_2O$ , dimethylsulfoxide (DMSO), or methanol.

### 2.2. Cell viability

Hepatocyte viability was assessed microscopically by plasma membrane disruption as determined by the trypan blue (0.1%, w/v) exclusion test [6]. Hepatocyte viability was determined every 30 min during the first hour and then at 2 and 3 h incubation, and the cells were at least 85–95% viable before their use.

### 2.3. $H_2O_2$ generating system

Following its addition to hepatocytes,  $H_2O_2$  is metabolised by catalase within a minute [13], therefore, a  $H_2O_2$  generating system was employed by adding glucose 10 mM to the hepatocyte suspension followed by glucose oxidase (1 U/mL). This system continuously supplied  $H_2O_2$  to the hepatocytes over a 3 h period, without affecting GSH levels.

### 2.4. Cellular NADPH Levels

NADPH levels were measured by high-pressure liquid chromatography (HPLC) using the method outlined by Stocchi et al. [14]. NADPH was extracted from three identically treated hepatocyte samples in 1 mL of 0.25 M potassium hydroxide. Potassium phosphate monobasic ( $KH_2PO_4$ , 100  $\mu$ L of 1 M) was added to the cell lysate. The cell lysates were then filtered using Amicon conical filtration membranes (Millipore Inc.) for 30 min at 1000  $\times$  g. The filtrate was passed through syringe filters and subjected to gradient HPLC analysis. The HPLC mobile phase was 100%  $KH_2PO_4$  (100 mM) for 5 min followed by a 10 min linear gradient to a phase consisting of 10% methanol and 90%  $KH_2PO_4$  (100 mM). Using these conditions, NADPH eluted at 8.3 min. Detection was carried out using UV absorption at 254 nm.

### 2.5. Cellular GSH and oxidized glutathione (GSSG) content

GSH and GSSG were measured by HPLC analysis of deproteinized samples (25% meta-phosphoric acid) after derivatization with iodoacetic acid and DNFB as per the method outlined by Reed et al. [15]. A Waters HPLC system (Model 150 pumps, WISP 710B auto injector and model 410 UV-vis detector) equipped with waters  $\mu$ Bondapak<sup>®</sup>  $NH_2$  (10  $\mu$ m) 3.9  $\times$  300 mm column was used. Detection was carried out using UV absorption at 364 nm.

### 2.6. Comet assay

The alkaline comet assay was performed as per the instructions supplied with the kit obtained from TRIVAGEN<sup>®</sup> (Catalog

# TA800). The heads and tails of the comets were scored using the CometScore<sup>®</sup> program. The amount of DNA damage was determined by scoring the heads and tails of the comets of 100 hepatocytes per treatment.

## 2.7. ROS formation

The rate of hepatocyte ROS generation induced by  $\alpha$ -oxoaldehydes was determined by adding DCFH-DA to the hepatocyte incubate. DCFH-DA penetrates hepatocytes and becomes hydrolyzed to form non-fluorescent dichlorofluorescein. Dichlorofluorescein then reacts with 'ROS' to form the highly fluorescent dichlorofluorescein that effluxes the cell. Aliquots (1 mL) were withdrawn at 15, 45 and 90 min after incubation with  $\alpha$ -oxoaldehydes. These samples were then centrifuged for 1 min at  $50 \times g$ . The cells were resuspended in 1 mL of Krebs-Henseleit media containing 1.6  $\mu$ M DCFD-DA. The cells were allowed to incubate at 37 °C for 10 min. The fluorescence intensity of dichlorofluorescein was measured using a Shimadzu RF5000U fluorescence spectrophotometer. Excitation and emission wavelengths were 500 and 520 nm, respectively [16].

## 2.8. H<sub>2</sub>O<sub>2</sub> measurement

H<sub>2</sub>O<sub>2</sub> was measured in hepatocytes by taking samples at 2', 5', 15', 30' and 60' using the FOX 1 reagent (ferrous oxidation of xylenol orange). The FOX 1 reagent consisted of 25 mM sulfuric acid, 250  $\mu$ M ferrous ammonium sulfate, 100  $\mu$ M xylenol orange and 0.1 M sorbitol. At the given time intervals 50  $\mu$ L of hepatocytes ( $1.0 \times 10^6$  cells/mL) were added to 950  $\mu$ L FOX 1 reagent and incubated for 30 min at room temperature. The absorbances of the samples were read at 560 nm [13].

## 2.9. Carbonylation assay

Total protein-bound carbonyl content was measured by derivatizing the carbonyl adducts with DNPH. Briefly an aliquot of the suspension of cells (0.5 mL,  $0.5 \times 10^6$  cells) was added to an equivalent volume (0.5 mL) of 0.1% DNPH (w/v) in 2.0N HCl and allowed to incubate for an hour at room temperature with vortexing every 15 min. This reaction was terminated and total cellular protein precipitated by the addition of an equivalent 1.0 mL volume of 20% TCA (w/v). Cellular protein was rapidly pelleted by centrifugation at 10,000 rpm, and the supernatant was discarded. Excess unincorporated DNPH was extracted three times using an excess volume (0.5 mL) of ethanol: ethyl acetate (1:1) solution. Following the extraction, the recovered cellular protein was dried under a stream of nitrogen and solubilized in 1 mL of Tris-buffered 8.0 M guanidine-HCl, pH 7.2. The resulting solubilized hydrazones were measured at 366–370 nm [17].

## 2.10. Mitochondrial membrane potential assay

The uptake and retention of the cationic fluorescent dye, rhodamine 123, has been used for the estimation of mitochondrial membrane potential. This assay is based on the fact that rhodamine 123 accumulates selectively in the mitochondria by facilitated diffusion. However, when the mitochondrial potential is decreased, the amount of rhodamine 123 that

enters the mitochondria is decreased as there is no facilitated diffusion. Thus the amount of rhodamine 123 in the supernatant is increased and the amount in the pellet is decreased.

Samples (500  $\mu$ L) were taken from the cell suspension incubated at 37 °C, and centrifuged at 1000 rpm for 1 min. The cell pellet was then resuspended in 2 mL of fresh incubation medium containing 1.5  $\mu$ M rhodamine 123 and incubated at 37 °C in a thermostatic bath for 10 min with gentle shaking. Hepatocytes were separated by centrifugation and the amount of rhodamine 123 appearing in the incubation medium was measured fluorimetrically using Shimadzu RF5000U fluorescence spectrophotometer set at 490 nm excitation and 520 nm emission wavelengths. The capacity of mitochondria to take up the rhodamine 123 was calculated as the difference in fluorescence intensity between control and treated cells [6].

## 2.11. Glyoxal metabolism

Glyoxal levels in isolated rat hepatocytes were measured as per the methods outlined by Okado-Matsumoto and Fridovich [18]. Briefly, 1',2'-diaminobenzene was used as a derivatizing agent for the analysis of glyoxal by isocratic gradient HPLC (solvent composition remains the same throughout the analysis). To a 1 mL sample of cells ( $1 \times 10^6$  cells), 0.2 mL of 5 M HClO<sub>4</sub>, 0.2 mL of 2,3-dimethylquinoxaline (as an internal standard), 0.2 mL of 10 mM 1',2'-diaminobenzene, and water were added to a final volume of 2 mL. After 1 h at 25 °C, HPLC analysis was performed. The column was a 5  $\mu$ m, 250  $\times$  4 mm RP-18 (Merck LiChrospher). The mobile phase was 50% (v/v) 25 mM ammonium formate buffer, pH 3.4, and 50% (v/v) methanol. A volume of 100  $\mu$ L was injected. The flow rate was 1.0 mL/min and quinoxalines were detected at 315 nm.

## 2.12. Statistical analysis

Statistical analysis was preformed by a one-way ANOVA test and significance was assessed by employing Tukey's post hoc test.

---

# 3. Results

## 3.1. Effect of glyoxal versus glyoxal metabolites on hepatocyte H<sub>2</sub>O<sub>2</sub> susceptibility

As shown in Table 1, 10  $\mu$ M glyoxal caused a marked increase in hepatocyte susceptibility to H<sub>2</sub>O<sub>2</sub> generated at a rate that did not cause cytotoxicity to control hepatocytes. This glyoxal concentration was far below the LD<sub>50</sub> concentration of 5 mM (the concentration required to cause 50% hepatocyte cytotoxicity in 2 h) [6]. Hepatocyte susceptibility to H<sub>2</sub>O<sub>2</sub> increased with increasing doses of glyoxal.

However, when hepatocytes were pre-incubated with glyoxal for 30 min to allow for glyoxal metabolism there was no effect on H<sub>2</sub>O<sub>2</sub> cytotoxicity. Furthermore, glyoxal metabolites such as glycolate and glyoxylate at 10  $\mu$ M did not significantly increase hepatocyte susceptibility to H<sub>2</sub>O<sub>2</sub>. A 50 times higher dose of glycolaldehyde was needed to increase hepatocyte H<sub>2</sub>O<sub>2</sub> susceptibility as compared to glyoxal. Furthermore, when glyoxal metabolism by oxido-reductases was

**Table 1 – Hepatocyte susceptibility to H<sub>2</sub>O<sub>2</sub> toxicity is markedly increased by glyoxal**

Treatment	Cytotoxicity (% trypan blue uptake)		
	60 min	120 min	180 min
Control hepatocyte	24 ± 4	28 ± 3	25 ± 5
+H <sub>2</sub> O <sub>2</sub> generating system	32 ± 5	39 ± 5	43 ± 6
+Glyoxal 5 µM	28 ± 5	42 ± 3	49 ± 4
+Glyoxal 10 µM	43 ± 6 <sup>a,b</sup>	66 ± 4 <sup>a,b,c</sup>	74 ± 5 <sup>a,b,c</sup>
+Aminoguanidine 10 mM (30' pre-incubation)	28 ± 5 <sup>d</sup>	32 ± 4 <sup>d</sup>	39 ± 3 <sup>d</sup>
+D-Penicillamine 1 mM (30' pre-incubation)	32 ± 4 <sup>d</sup>	36 ± 5 <sup>d</sup>	40 ± 7 <sup>d</sup>
+Sorbinil 100 µM (30' pre-incubation)	50 ± 3	100 <sup>a,b</sup>	100 <sup>a,b</sup>
+Glyoxal 10 µM (30' pre-incubation)	25 ± 3	26 ± 5	28 ± 3
+Glyoxal 100 µM	37 ± 5	80 ± 4 <sup>a,c</sup>	100 <sup>a,c</sup>
+Glyoxal 500 µM	46 ± 3	100 <sup>a,c</sup>	100 <sup>a,c</sup>
+Glycoladehyde 500 µM	25 ± 6	56 ± 6 <sup>a,c</sup>	70 ± 4 <sup>a,c</sup>
+Glycollate 500 µM	27 ± 3 <sup>d</sup>	34 ± 4 <sup>d</sup>	33 ± 6 <sup>d</sup>
+Glyoxylate 500 µM	26 ± 3 <sup>d</sup>	27 ± 4 <sup>d</sup>	30 ± 4 <sup>d</sup>
+Ethylene glycol 500 µM	29 ± 4 <sup>d</sup>	36 ± 3 <sup>d</sup>	32 ± 5 <sup>d</sup>
+Sorbinil 100 µM	34 ± 2	33 ± 6 <sup>d</sup>	38 ± 5 <sup>d</sup>
+Glyoxal 10 µM	29 ± 4	27 ± 5	26 ± 3
+Aminoguanidine 10 mM (30' pre-incubation)	25 ± 4	28 ± 6	24 ± 5
+D-Penicillamine 1 mM (30' pre-incubation)	26 ± 7	24 ± 7	31 ± 7
+Sorbinil 100 µM (30' pre-incubation)	23 ± 5	27 ± 6	26 ± 5

Isolated rat hepatocytes were incubated at 37 °C in rotating round bottom flasks with 95% O<sub>2</sub> and 5% CO<sub>2</sub> in Krebs–Henseleit buffer (pH 7.4). Hepatocyte viability was assessed microscopically by plasma membrane disruption as determined by the trypan blue (0.1%, w/v) exclusion test (n = 3).

<sup>a</sup> Significant difference as compared to the control ( $p < 0.05$ ).

<sup>b</sup> Significant as compared to glyoxal 10 µM alone ( $p < 0.05$ ).

<sup>c</sup> Significant as compared to H<sub>2</sub>O<sub>2</sub> generating system ( $p < 0.005$ ).

<sup>d</sup> Significant as compared to H<sub>2</sub>O<sub>2</sub> generating system + glyoxal 10 µM ( $p < 0.05$ ).

inhibited by sorbinil (a specific aldose reductase inhibitor), H<sub>2</sub>O<sub>2</sub> toxicity increased even further with 10 µM glyoxal. Glyoxal traps such as D-penicillamine and aminoguanidine prevented the glyoxal-enhanced H<sub>2</sub>O<sub>2</sub> toxicity.

### 3.2. Effect of glyoxal on H<sub>2</sub>O<sub>2</sub>-induced hepatocyte GSH oxidation

As shown in Fig. 1, 10 µM glyoxal markedly increased H<sub>2</sub>O<sub>2</sub>-induced hepatocyte GSH depletion and GSSG formation. H<sub>2</sub>O<sub>2</sub> generating system depleted 50% of the GSH over a 90 min period (Fig. 1b), but in the presence of glyoxal, this level of GSH depletion was reached within 15 min. The control sample containing vehicle alone exhibited little GSH or oxidation depletion over the incubation period of 90 min.

### 3.3. Effect of glyoxal on H<sub>2</sub>O<sub>2</sub>-induced NADPH depletion

Hepatocyte NADPH depletion by H<sub>2</sub>O<sub>2</sub> was markedly increased when hepatocytes were treated with glyoxal (Table 2). Hepatocytes treated with glyoxal and the H<sub>2</sub>O<sub>2</sub> generating system had 167 ± 15 nM NADPH as compared to 467 ± 18 nM of control or 359 ± 23 nM of the H<sub>2</sub>O<sub>2</sub> generating system by itself. There was approximately a 65% decrease in cellular NADPH levels when H<sub>2</sub>O<sub>2</sub> stressed hepatocytes were treated with 10 µM glyoxal.

### 3.4. Effect of glyoxal on H<sub>2</sub>O<sub>2</sub>-induced hepatocyte protein oxidation

In the presence of glyoxal, hepatocyte protein carbonyl formation induced by H<sub>2</sub>O<sub>2</sub> was further increased (Fig. 2).

Within 30 min there was an increase in protein oxidation in hepatocytes treated with glyoxal and the H<sub>2</sub>O<sub>2</sub> generating system (21 ± 2 nmol/1.0 × 10<sup>6</sup> cells) as compared to control (12 ± 0.5 nmol/1.0 × 10<sup>6</sup> cells) and the H<sub>2</sub>O<sub>2</sub> generating system by itself (14 ± 1.5 nmol/1.0 × 10<sup>6</sup> cells). Overtime the hepatocytes treated with glyoxal and the H<sub>2</sub>O<sub>2</sub> generating system showed a marked increase in protein oxidation as compared to the control or the H<sub>2</sub>O<sub>2</sub> generating system alone. The level of protein oxidation increased significantly before cytotoxicity ensued.

### 3.5. Effect of glyoxal on H<sub>2</sub>O<sub>2</sub>-induced hepatocyte decrease in mitochondrial membrane potential

As shown in Fig. 3, addition of 10 µM glyoxal caused a marked decrease in hepatocyte mitochondrial membrane potential induced by H<sub>2</sub>O<sub>2</sub>, which occurred before cytotoxicity ensued. Membrane potential was restored when fructose 10 mM (ATP generator) was added to the hepatocytes 45 min after incubation with the H<sub>2</sub>O<sub>2</sub> generating system suggesting that the mitochondrial potential decrease was reversible.

### 3.6. Preventing the oxidative stress and cytotoxicity induced by glyoxal plus H<sub>2</sub>O<sub>2</sub>

Increased ROS production and cellular H<sub>2</sub>O<sub>2</sub> levels occurred at 90 min and 60 min, respectively (Table 3). 10 µM glyoxal was ~97% metabolised within 120 min. However, glyoxal metabolism was inhibited in the presence of the H<sub>2</sub>O<sub>2</sub> generating system. Furthermore, there was a significant



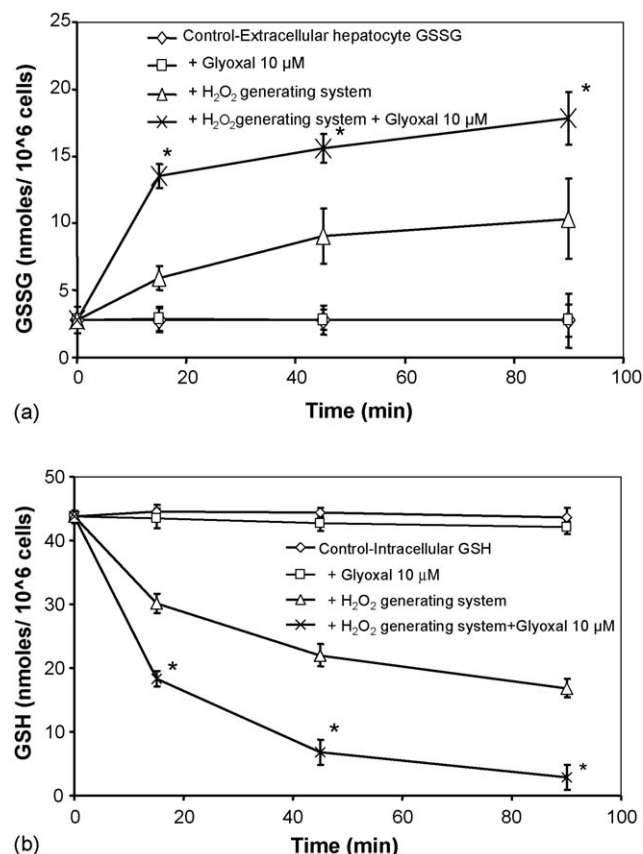


**Fig. 1 – Glyoxal increased hepatocyte GSH oxidation induced by H<sub>2</sub>O<sub>2</sub>.** (a) Accumulation of extracellular GSSG formation and (b) intracellular GSH depletion. Isolated rat hepatocytes were incubated at 37 °C in rotating round bottom flasks with 95% O<sub>2</sub> and 5% CO<sub>2</sub> in Krebs–Henseleit buffer (pH 7.4). GSH and GSSG were measured by conjugation with 2,4-dinitrofluorobenzene (DNFB) using isocratic gradient HPLC ( $n = 3$ ). \*Significant difference as compared to H<sub>2</sub>O<sub>2</sub> generating system ( $p < 0.05$ ).

increase in DNA damage as measured by the comet assay at 120 min. Quercetin (antioxidant), propyl gallate (antioxidant), desferoxamine (iron chelator) and fructose (ATP generator) decreased cytotoxicity, ROS formation and decreased cellular H<sub>2</sub>O<sub>2</sub> levels. The lipid peroxidation byproduct, acrolein, caused an increase in hepatocyte susceptibility to H<sub>2</sub>O<sub>2</sub> and ROS production as compared to the H<sub>2</sub>O<sub>2</sub> generating system alone.

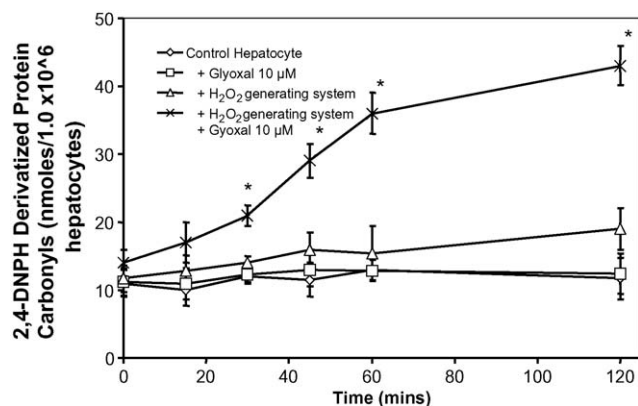


**Fig. 2 – Glyoxal increased hepatocyte protein oxidation induced by H<sub>2</sub>O<sub>2</sub>.** Isolated rat hepatocytes were incubated at 37 °C in rotating round bottom flasks with 95% O<sub>2</sub> and 5% CO<sub>2</sub> in Krebs–Henseleit buffer (pH 7.4). Total protein-bound carbonyl content was measured by derivatizing the carbonyl adducts with 2,4-dinitrophenylhydrazine (DNPH) and measuring the hydrazone formation in the extracted protein fraction at 366–370 nm ( $n = 3$ ). \*Significant difference as compared to H<sub>2</sub>O<sub>2</sub> generating system ( $p < 0.05$ ).

#### 4. Discussion

Hepatocytes are very resistant to H<sub>2</sub>O<sub>2</sub> (particularly if it is added as a bolus) largely because of their high catalase activity, GSH levels, GSH peroxidase and GSH reductase activities. Indeed concentrations of 20 mM H<sub>2</sub>O<sub>2</sub> are not cytotoxic. When a slow H<sub>2</sub>O<sub>2</sub> generating system is used, catalase is much less effective at decomposing H<sub>2</sub>O<sub>2</sub>. Generating approximately 3 mM H<sub>2</sub>O<sub>2</sub> per hour caused barely detectable cytotoxicity in 2 h. However, as little as 10  $\mu$ M glyoxal was sufficient to increase hepatocyte susceptibility to non-cytotoxic concentrations of H<sub>2</sub>O<sub>2</sub> (Table 1). Previously we found that the glyoxal concentration required to cause cytotoxicity in isolated rat hepatocytes in the absence of exogenous H<sub>2</sub>O<sub>2</sub> was 5 mM [6]. The glyoxal effect was dependent on the glyoxal concentration and was lost if the H<sub>2</sub>O<sub>2</sub> generating system was added 30 min after the glyoxal. The concentration of glyoxal in human tissue and body fluids is generally low (eg. ~12.5  $\mu$ g/mL in human blood)[19]. The low concentration of glyoxal is maintained as a result of the

**Table 2 – H<sub>2</sub>O<sub>2</sub>-induced hepatocyte NADPH depletion is increased by glyoxal**

Treatment	Hepatocyte NADPH levels (nmol/10 <sup>6</sup> cells) 90 min
Control	467 $\pm$ 18
+Glyoxal 10 $\mu$ M	454 $\pm$ 32
+H <sub>2</sub> O <sub>2</sub> generating system	359 $\pm$ 23
+Glyoxal 10 $\mu$ M	167 $\pm$ 15 <sup>a</sup>

Isolated rat hepatocytes were incubated at 37 °C in rotating round bottom flasks with 95% O<sub>2</sub> and 5% CO<sub>2</sub> in Krebs–Henseleit buffer (pH 7.4). NADPH levels were measured by HPLC. NADPH was extracted from three identically treated hepatocytes samples. NADPH eluted at 8.3 min. Detection was carried out using UV absorption at 254 nm ( $n = 3$ ).

<sup>a</sup> Significant difference as compared to the H<sub>2</sub>O<sub>2</sub> generating system ( $p < 0.05$ ).

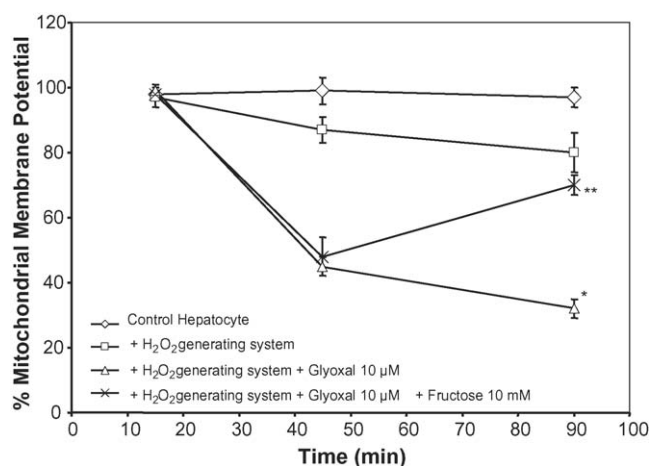


**Fig. 3 – Glyoxal markedly increased the H<sub>2</sub>O<sub>2</sub>-induced collapse of the hepatocyte mitochondrial membrane potential.** Isolated rat hepatocytes were incubated at 37 °C in rotating round bottom flasks with 95% O<sub>2</sub> and 5% CO<sub>2</sub> in Krebs–Henseleit buffer (pH 7.4). Rhodamine 123 was used to assess mitochondrial membrane potential. Fluorimetric measurements were made at  $\lambda_{\text{excitation}} = 490 \text{ nm}$   $\lambda_{\text{emission}} = 520 \text{ nm}$ . Fructose was added 45 min after the H<sub>2</sub>O<sub>2</sub> generating system and glyoxal ( $n = 3$ ). \*Significant difference as compared to H<sub>2</sub>O<sub>2</sub> generating system ( $p < 0.05$ ) and \*\*significant difference as compared to H<sub>2</sub>O<sub>2</sub> generating system + glyoxal 10 μM ( $p < 0.05$ ).

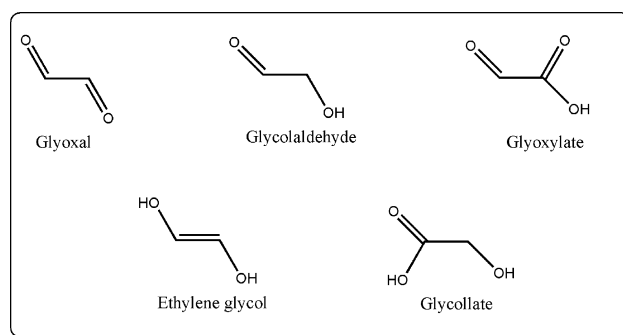


**Fig. 4 – Structures of glyoxal and its metabolites.**

enzymatic detoxification of glyoxal. Elevated levels of glyoxal are observed in oxidative stress related diseases such as diabetes ( $\sim 27.2 \mu\text{g/mL}$ ) [19]. Diabetes results in oxidative stress which is evident by the decrease in red blood cell GSH concentration; therefore, there is a consequent decrease in MG and glyoxal detoxification. Accumulation of glyoxals has been implicated in chronic clinical complications associated with diabetes mellitus via AGE formation and activation of pro-inflammatory response by monocytes/macrophages [19,20]. Therefore, the relationship between glyoxal and oxidative stress (H<sub>2</sub>O<sub>2</sub>) on cellular toxicity was investigated.

The glyoxal metabolites, glyoxylate, glycolate, and glycolaldehyde (Fig. 4) were also much less effective at increasing hepatocyte H<sub>2</sub>O<sub>2</sub> susceptibility. Therefore, the increased H<sub>2</sub>O<sub>2</sub> toxicity observed with glyoxal was due to glyoxal itself and not its metabolites. Glycolaldehyde at 500 μM also increased

**Table 3 – Glyoxal increased cytotoxicity, ROS formation, oxidative DNA damage induced by oxidative stress (H<sub>2</sub>O<sub>2</sub>)**

Treatments	Cytotoxicity (% Trypan Blue uptake)	Cellular ROS formation (FI units)	Cellular H <sub>2</sub> O <sub>2</sub> measurement (mM)	Cellular DNA damage tail moment/ 100 cells (comet score)	% Glyoxal
	120 min	90 min	60 min	90 min	120 min
Control-hepatocyte	23 ± 4	43 ± 14	0	14 ± 2	n/a
+Glyoxal 10 μM	25 ± 3	46 ± 11	0	18 ± 3	3 ± 2
+H <sub>2</sub> O <sub>2</sub> generating system	39 ± 5 <sup>a</sup>	110 ± 21 <sup>a</sup>	3.61 ± 0.61 <sup>a</sup>	43 ± 5 <sup>a</sup>	n/a
+Glyoxal 10 μM	66 ± 4 <sup>b,c</sup>	310 ± 39 <sup>b,c</sup>	4.91 ± 0.19 <sup>b,c</sup>	79 ± 8 <sup>b,c</sup>	80 ± 7 <sup>a,b</sup>
+Quercetin 100 μM	32 ± 7 <sup>d</sup>	57 ± 19 <sup>d</sup>	0.59 ± 0.21 <sup>d</sup>	–	n/d
+Desferoxamine 300 μM	43 ± 7 <sup>d</sup>	49 ± 12 <sup>d</sup>	0.79 ± 0.36 <sup>d</sup>	–	n/d
+Propyl gallate 50 μM	37 ± 5 <sup>d</sup>	63 ± 22 <sup>d</sup>	0.83 ± 0.23 <sup>d</sup>	–	n/d
+ Fructose 10 mM	41 ± 6 <sup>d</sup>	73 ± 13 <sup>d</sup>	0.69 ± 0.19 <sup>d</sup>	–	n/d
+Acrolein 20 μM	50 ± 5 <sup>a,c</sup>	195 ± 19 <sup>a,c</sup>	4.23 ± 0.32 <sup>a,c</sup>	–	n/d

Isolated rat hepatocytes were incubated at 37 °C in rotating round bottom flasks with 95% O<sub>2</sub> and 5% CO<sub>2</sub> in Krebs–Henseleit buffer (pH 7.4). Hepatocyte viability was assessed microscopically by plasma membrane disruption as determined by the trypan blue (0.1%, w/v) exclusion test. ROS-fluorimetric measurements were made of 2',7'-dichlorofluorescein oxidation at  $\lambda_{\text{excitation}} = 500 \text{ nm}$   $\lambda_{\text{emission}} = 520 \text{ nm}$ . H<sub>2</sub>O<sub>2</sub> measurement — FOX 1 reagent (ferrous oxidation of xylenol orange) was used to measure H<sub>2</sub>O<sub>2</sub>. The absorbances of the samples were read at 560 nm. DNA damage — the alkaline comet assay was performed as per the instructions supplied with the kit obtained from TRIVAGEN<sup>®</sup> Catalog # TA800. The heads and tails of the comets were scored using the CometScore<sup>®</sup> program. The amount of DNA damage was determined by scoring the heads and tails of the comets of 100 hepatocytes per treatment. Glyoxal levels — 1',2'-diaminobenzene was used as a derivatizing agent for the analysis of glyoxal by isocratic gradient HPLC. H<sub>2</sub>O<sub>2</sub> generating system: H<sub>2</sub>O<sub>2</sub> generating system, (–) not measured, n/a: not applicable, n/d: not determined ( $n = 3$ ).

<sup>a</sup> Significant difference as compared to the control ( $p < 0.05$ ).

<sup>b</sup> Significant as compared to glyoxal 10 μM alone ( $p < 0.05$ ).

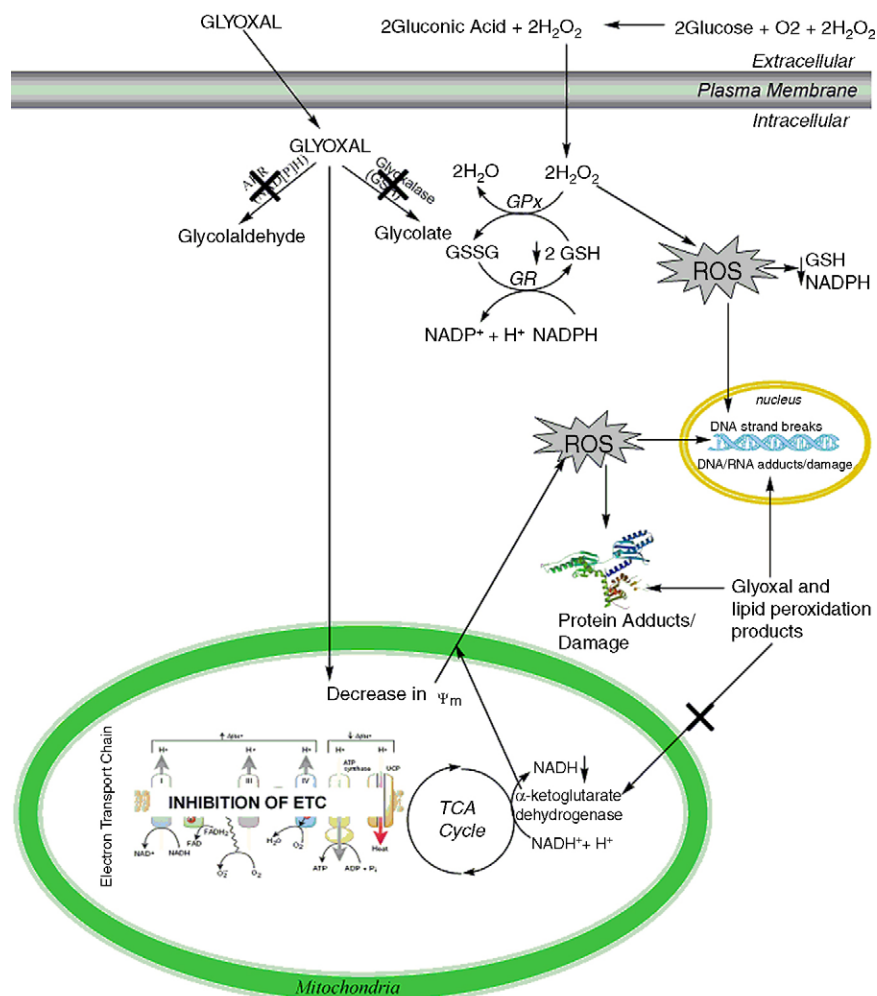
<sup>c</sup> Significant as compared to H<sub>2</sub>O<sub>2</sub> generating system ( $p < 0.05$ ).

<sup>d</sup> Significant as compared to H<sub>2</sub>O<sub>2</sub> generating system + glyoxal 10 μM ( $p < 0.01$ ).

hepatocyte susceptibility to  $\text{H}_2\text{O}_2$ . Furthermore, glycolaldehyde is oxidized by superoxide radicals to form glyoxal and  $\text{H}_2\text{O}_2$  [21]. Thus the increased susceptibility of hepatocytes to  $\text{H}_2\text{O}_2$  in the presence of glycolaldehyde maybe due to its conversion to glyoxal. Furthermore, when hepatocyte aldose reductase was inhibited by its specific inhibitor sorbinil, glyoxal effectiveness at increasing  $\text{H}_2\text{O}_2$  toxicity was further increased. Sorbinil on its own did not increase  $\text{H}_2\text{O}_2$  toxicity. Furthermore, glyoxal-induced  $\text{H}_2\text{O}_2$  cytotoxicity was prevented by glyoxal traps such as D-penicillamine and amino-guanidine. These results indicate that glyoxal itself was responsible for the increased hepatocyte susceptibility to  $\text{H}_2\text{O}_2$ .

To further understand how glyoxal increased  $\text{H}_2\text{O}_2$  cytotoxicity, hepatocellular GSH levels were measured (Fig. 1). As mentioned before, oxidative stress and  $\alpha$ -oxoaldehyde metabolism have overlapping requirements for GSH and NADPH. GSH not only forms the primary defense mechanism of the cell against oxidative stress, but is essential for glyoxal and MG metabolism by the glyoxalase

system [10]. However, when the concentration of GSH decreases below 3 mM in the liver (normally 15 mM), the NAD(P)H dependent oxido-reductase system becomes the primary detoxification mechanism for these  $\alpha$ -oxoaldehydes [22]. Glyoxal by itself even at 100  $\mu\text{M}$  (data not shown) did not affect hepatocyte GSH levels. However, glyoxal at 10  $\mu\text{M}$  markedly increased hepatocyte GSH oxidation to GSSG by  $\text{H}_2\text{O}_2$ . GSH depletion caused an increase in cellular  $\text{H}_2\text{O}_2$  levels (Table 3). This could occur because glyoxal can inhibit  $\text{H}_2\text{O}_2$  removal by the GSH peroxidase/GSH reductase/NADPH pathway. Previously, we showed that glyoxal inactivated GSH reductase [6]. NADPH generating enzymes such as cytosolic glucose-6-phosphate dehydrogenase (G6PDH) and mitochondrial isocitrate dehydrogenase (ICDH) were also inhibited by glyoxal [23] and would inhibit GSH regeneration thus compromising hepatocyte  $\text{H}_2\text{O}_2$  detoxification. G6PDH and ICDH activities may also be impaired by glyoxal because glyoxal diminishes the availability of NADPH for these enzymes. Furthermore, inhibition by glyoxal and  $\text{H}_2\text{O}_2$  of the rate limiting enzymes in the pentose phosphate/glyco-



**Scheme 1 – Mechanism of glyoxal-induced increased  $\text{H}_2\text{O}_2$  cytotoxicity.**  $\text{H}_2\text{O}_2$  caused a decrease in cellular GSH and NADPH which inhibited glyoxal metabolism. Glyoxal causes inhibition of essential cellular proteins like GSH reductase/peroxidase,  $\alpha$ -ketoglutarate dehydrogenase and thioredoxin reductase. Glyoxal causes a decrease in mitochondrial membrane potential ( $\psi_m$ ) by partially inhibiting the mitochondrial electron transport chain (ETC) resulting in increased mitochondrial reactive oxygen species (ROS) formation. Glyoxal also causes protein carbonylation/oxidation and DNA oxidation.

lytic pathway and the mitochondrial citric acid cycle/respiratory chain could also explain a compromised hepatocyte NADPH supply. The comparative enzyme susceptibility in isolated mitochondria to 50  $\mu$ M  $H_2O_2$  was aconitase > succinate dehydrogenase > isocitrate dehydrogenase >  $\alpha$ -ketoglutarate dehydrogenase > Complex I and glyceraldehyde-3-phosphate dehydrogenase [24]. Inhibition of the mitochondrial NADH supply by inhibiting  $\alpha$ -ketoglutarate dehydrogenase with  $H_2O_2$  could also affect NADPH formation catalysed by transhydrogenase [25].

The  $H_2O_2$  generating system or glyoxal alone in the quantities used in this study were insufficient in influencing the GSH levels in the hepatocytes. However, together they depleted cellular GSH, which could impair detoxification of glyoxal by the glyoxalase system [11,22]. This is indirectly supported by the results shown in Table 3 whereby  $H_2O_2$  prevented glyoxal disappearance allowing glyoxal to inactivate enzymes involved in the metabolism of  $H_2O_2$  and carbonyls. The inactivation of these enzymes could be a result of protein carbonylation/oxidation (Fig. 2).

It has also been shown that GSH depletion facilitates lipid peroxidation which can initiate oxidative stress [26]. Therefore, we measured ROS formation together with  $H_2O_2$  levels (Table 3) and found that glyoxal markedly increased  $H_2O_2$ -induced hepatocyte ROS formation, and increased cellular  $H_2O_2$  levels. Furthermore, antioxidants such as quercetin, desferoxamine (iron chelator) and propyl gallate decreased ROS formation and cytotoxicity. The increased ROS could also result from impaired mitochondrial activity as indicated by the decreased mitochondrial membrane potential (Fig. 3). However, the mitochondria were not irreversibly damaged as incubation with fructose (a glycolytic ATP generator) restored mitochondrial membrane potential and decreased ROS and cytotoxicity.

Protection against oxidative DNA damage in the cell is a result of enzymatic and non-enzymatic antioxidants that neutralize or detoxify ROS (e.g. GSH peroxidase, GSH, catalase, etc.). Protection against glycation by reactive  $\alpha$ -oxoaldehydes is due to the glyoxalase system and oxido-reductases [27]. However, in our system, both the cellular antioxidant defenses (i.e. GSH) and  $\alpha$ -oxoaldehyde detoxification system were compromised thus causing an increase in DNA oxidative damage (Table 3).

We tested acrolein as like glyoxal it is also a lipid peroxidation byproduct [6,28,29]. Acrolein is a highly reactive  $\alpha,\beta$ -unsaturated aldehyde that readily alkylates nucleophilic centers in biomolecules (eg. lysine, arginines and cysteines in proteins)[30]. Acrolein at 20  $\mu$ M increased hepatocyte susceptibility to  $H_2O_2$  which could be due to the strong cross-linking potency of acrolein. Acrolein adducts retain carbonyl groups that readily react with neighboring nucleophiles in the same or adjacent macromolecules [30–34].

Scheme 1 outlines a mechanism proposed for the effect of glyoxal on hepatocyte  $H_2O_2$  susceptibility. Detoxification of  $H_2O_2$  caused hepatocyte GSH and NADPH depletion which in turn inhibited glyoxal metabolism. Increased cellular levels of glyoxal caused an increase in protein carbonylation/oxidation resulting in inhibition of essential cellular enzymes like GSH reductase and peroxidase. Glyoxal may partly inhibit the mitochondrial electron transport chain resulting in increased

mitochondrial ROS formation as the mitochondrial membrane potential was decreased. Furthermore, glyoxal enhanced DNA damage caused by  $H_2O_2$ .

To our knowledge this is the first study that illustrates an apparent synergism between glyoxal and  $H_2O_2$ -induced cytotoxicity. Both glyoxal detoxification and cellular antioxidant defenses require reducing equivalents such as NADPH and GSH. Therefore, under conditions of oxidative stress the cell is more vulnerable to glyoxal and  $H_2O_2$  due to a decrease in its primary antioxidant defenses and reducing equivalents. Understanding the mechanism of this synergistic toxicity will enable us to develop novel drug therapies for diseases such as complications associated with diabetes which results in oxidative stress, Parkinson's disease and Alzheimer's disease to name a few.

## Acknowledgements

This research has been funded by the Natural Sciences and Engineering Research Council of Canada grant #: RGPIN 3783-03. Nandita Shangari is the recipient of a postgraduate fellowship from NSERC. Tom S. Chan is the recipient of Canadian Association for the Study of the Liver and Canadian Institutes for Health Research.

## REFERENCES

- [1] Grosjean D. Particulate carbon in Los Angeles air. *Sci Total Environ* 1984;32:133–45.
- [2] O'Brien PJ, Siraki AG, Shangari N. Aldehyde sources, metabolism, molecular toxicity mechanisms, and possible effects on human health. *Crit Rev Toxicol* 2005;35:609–62.
- [3] Shangari N, Bruce WR, Poon R, O'Brien PJ. Toxicity of glyoxals — role of oxidative stress, metabolic detoxification and thiamine deficiency. *Biochem Soc Trans* 2003;31: 1390–3.
- [4] Thornalley PJ, Jahan I, Ng R. Suppression of the accumulation of triosephosphates and increased formation of methylglyoxal in human red blood cells during hyperglycaemia by thiamine in vitro. *J Biochem (Tokyo)* 2001;129:543–9.
- [5] Wells-Knecht KJ, Zyzak DV, Litchfield JE, Thorpe SR, Baynes JW. Mechanism of autooxidative glycosylation: identification of glyoxal and arabinose as intermediates in the autooxidative modification of proteins by glucose. *Biochemistry* 1995;34:3702–9.
- [6] Shangari N, O'Brien PJ. The cytotoxic mechanism of glyoxal involves oxidative stress. *Biochem Pharmacol* 2004;68:1433–42.
- [7] Frye EB, Degenhardt TP, Thorpe SR, Baynes JW. Role of the Maillard reaction in aging of tissue proteins. Advanced glycation end product-dependent increase in imidazolium cross-links in human lens proteins. *J Biol Chem* 1998;273:18714–9.
- [8] Westwood ME, Argirov OK, Abordo EA, Thornalley PJ. Methylglyoxal-modified arginine residues — a signal for receptor-mediated endocytosis and degradation of proteins by monocytic THP-1 cells. *Biochim Biophys Acta* 1997;1356:84–94.
- [9] Roberts MJ, Wondrak GT, Laurean DC, Jacobson MK, Jacobson EL. DNA damage by carbonyl stress in human skin cells. *Mutat Res* 2003;522:45–56.



- [10] Abordo EA, Minhas HS, Thornalley PJ. Accumulation of alpha-oxoaldehydes during oxidative stress: a role in cytotoxicity. *Biochem Pharmacol* 1999;58:641–8.
- [11] Vander Jagt DL, Robinson B, Taylor KK, Hunsaker LA. Reduction of trioses by NADPH-dependent aldo-keto reductases. Aldose reductase, methylglyoxal, and diabetic complications. *J Biol Chem* 1992;267:4364–9.
- [12] Moldeus P, Hogberg J, Orrenius S. Isolation and use of liver cells. *Meth Enzymol* 1978;52:60–71.
- [13] Ou P, Wolff SP. A discontinuous method for catalase determination at 'near physiological' concentrations of H<sub>2</sub>O<sub>2</sub> and its application to the study of H<sub>2</sub>O<sub>2</sub> fluxes within cells. *J Biochem Biophys Meth* 1996;31:59–67.
- [14] Stocchi V, Cucchiari L, Magnani M, Chiarantini L, Palma P, Crescentini G. Simultaneous extraction and reverse-phase high-performance liquid chromatographic determination of adenine and pyridine nucleotides in human red blood cells. *Anal Biochem* 1985;146:118–24.
- [15] Reed DJ, Babson JR, Beatty PW, Brodie AE, Ellis WW, Potter DW. High-performance liquid chromatography analysis of nanomole levels of glutathione, glutathione disulfide, and related thiols and disulfides. *Anal Biochem* 1980;106:55–62.
- [16] Pourahmad J, O'Brien PJ. A comparison of hepatocyte cytotoxic mechanisms for Cu<sup>2+</sup> and Cd<sup>2+</sup>. *Toxicology* 2000;143:263–73.
- [17] Hartley DP, Kroll DJ, Petersen DR. Prooxidant-initiated lipid peroxidation in isolated rat hepatocytes: detection of 4-hydroxynonenal- and malondialdehyde-protein adducts. *Chem Res Toxicol* 1997;10:895–905.
- [18] Okado-Matsumoto A, Fridovich I. The role of alpha,beta-dicarbonyl compounds in the toxicity of short chain sugars. *J Biol Chem* 2000;275:34853–7.
- [19] Lapolla A, Flamini R, Dalla VA, Senesi A, Reitano R, Fedele D, et al. Glyoxal and methylglyoxal levels in diabetic patients: quantitative determination by a new GC/MS method. *Clin Chem Lab Med* 2003;41:1166–73.
- [20] Thornalley PJ. Glutathione-dependent detoxification of alpha-oxoaldehydes by the glyoxalase system: involvement in disease mechanisms and antiproliferative activity of glyoxalase I inhibitors. *Chem Biol Interact* 1998;111–112:137–51.
- [21] Thornalley PJ, Langborg A, Minhas HS. Formation of glyoxal, methylglyoxal and 3-deoxyglucosone in the glycation of proteins by glucose. *Biochem J* 1999;344 (Pt 1):109–16.
- [22] Vander Jagt DL, Hunsaker LA. Methylglyoxal metabolism and diabetic complications: roles of aldose reductase, glyoxalase-I, betaine aldehyde dehydrogenase and 2-oxoaldehyde dehydrogenase. *Chem Biol Interact* 2003;143–144:341–51.
- [23] Morgan PE, Dean RT, Davies MJ. Inactivation of cellular enzymes by carbonyls and protein-bound glycation/glycoxidation products. *Arch Biochem Biophys* 2002;403:259–69.
- [24] Nulton-Persson AC, Szveda LI. Modulation of mitochondrial function by hydrogen peroxide. *J Biol Chem* 2001;276:23357–61.
- [25] Tretter L, Adam-Vizi V. Inhibition of Krebs cycle enzymes by hydrogen peroxide: a key role of [alpha]-ketoglutarate dehydrogenase in limiting NADH production under oxidative stress. *J Neurosci* 2000;20:8972–9.
- [26] de Groot H, Brecht M. Reoxygenation injury in rat hepatocytes: mediation by O<sub>2</sub>/H<sub>2</sub>O<sub>2</sub> liberated by sources other than xanthine oxidase. *Biol Chem Hoppe Seyler* 1991;372:35–41.
- [27] Thornalley PJ. Protecting the genome: defence against nucleotide glycation and emerging role of glyoxalase I overexpression in multidrug resistance in cancer chemotherapy. *Biochem Soc Trans* 2003;31: 1372–7.
- [28] Kaminskas LM, Pyke SM, Burcham PC. Reactivity of hydrazinophthalazine drugs with the lipid peroxidation products acrolein and crotonaldehyde. *Org Biomol Chem* 2004;2:2578–84.
- [29] Luo J, Shi R. Acrolein induces axolemmal disruption, oxidative stress, and mitochondrial impairment in spinal cord tissue. *Neurochem Int* 2004;44:475–86.
- [30] Kaminskas LM, Pyke SM, Burcham PC. Strong protein adduct trapping accompanies abolition of acrolein-mediated hepatotoxicity by hydralazine in mice. *J Pharmacol Exp Ther* 2004;310:1010.
- [31] He Y, Nagano M, Yamamoto H, Miyamoto E, Futatsuka M. Modifications of neurofilament proteins by possible metabolites of allyl chloride in vitro. *Drug Chem Toxicol* 1995;18:315–31.
- [32] Kozekov ID, Nechev LV, Sanchez A, Harris CM, Lloyd RS, Harris TM. Interchain cross-linking of DNA mediated by the principal adduct of acrolein. *Chem Res Toxicol* 2001;14:1482–5.
- [33] Kurtz AJ, Lloyd RS. 1,N<sub>2</sub>-deoxyguanosine adducts of acrolein, crotonaldehyde, and trans-4-hydroxynonenal cross-link to peptides via Schiff base linkage. *J Biol Chem* 2003;278:5970–6.
- [34] Kuykendall JR, Bogdanffy MS. Efficiency of DNA-histone crosslinking induced by saturated and unsaturated aldehydes in vitro. *Mutat Res* 1992;283:131–6.